JOURNAL OF PROPULSION AND POWER
Vol. 13, No. 4, July–August 1997

Experimental Study on Rotating Cavitation of Rocket Propellant Pump Inducers

T. Hashimoto,* M. Yoshida,† and M. Watanabe‡
National Aerospace Laboratory, Kimigaya, Kakuda, Miyagi 981-15, Japan
K. Kamijo§
Tohoku University, Katahira, Sendai, Miyagi 980-77, Japan
and
Y. Tsujimoto¶
Osaka University, Toyonaka, Osaka 560, Japan

Research on rotating cavitation progressed during the development of a liquid oxygen (LOX) turbopump for the LE-7 engine of the H-II rocket. In some ranges of cavitation numbers, supersynchronous shaft vibrations were observed in the LE-7 LOX main pump inducer. From a comparison with the results of our previous studies it was concluded that such shaft vibrations were caused by rotating cavitation in the inducer. A simple modification of the inducer upstream housing almost completely extinguished such shaft vibrations. Some characteristics of rotating cavitation have been fairly well elucidated. However, we were not able to fully explain the mechanism of the influence of the simple modification of the inducer upstream housing on the rotating cavitation. We thus commenced further experimental studies to investigate rotating cavitation in more detail. In the present study, some visual observations of rotating cavitation were conducted using the same inducer test facility as that used in our previous work.

Introduction

AT the Kakuda Research Center of the National Aerospace Laboratory, cavitating inducer instability has been investigated for the past 20 years. At the beginning of this research, rotating cavitation was first explicitly identified in an experiment mainly using visual observations of three-bladed helical inducers for rocket propellant pumps.[1,2] It was clarified that the cavitating region rotated in the periphery of the inducer inlet at a higher rotating speed than that of the rotating blades in a certain range of flow coefficients and cavitation numbers, including the design point. This special feature is completely different from that of rotating stall, which occurs at a lower flow rate with positive slope of pressure performance, and the stalled region propagates slower than the rotational speed of the impeller. It was also clarified that rotating cavitation was a local flow instability restricted to the inducer inlet just the same as in the case of rotating stall. It should be mentioned that clarification of these specific features of rotating cavitation was facilitated by reference to studies[3–5] cited in our previous paper.[6]

During the development of the liquid oxygen (LOX) turbopump for the LE-7 engine of the H-II rocket, supersynchronous shaft vibrations occurred because of rotating cavitation in the inducer of the main pump.[6] The ratios of these vibration frequencies to the shaft rotating frequency were from 1.0 to 1.2. Efforts were made to solve this problem. Fortunately, we found a device to suppress the rotating cavitation.[6] A simple modification of the inducer upstream housing almost completely extinguished the supersynchronous shaft vibrations. It also extinguished the unstable head coefficient curve that was caused by the rotating cavitation and the steady asymmetrical cavitation, considered to be a kind of rotating cavitation. An outline of the suppression of rotating cavitation of the LE-7 LOX pump inducer is given in the Appendix.

Subsequently, we succeeded in developing an initial theory of rotating cavitation that explained the difference between rotating cavitation and rotating stall.[7] The theory showed that the cause of rotating cavitation was the positive mass flow gain factor, and that the damping rate of rotating cavitation disturbance and the propagating velocity were greatly affected by a combination of cavitation compliance and mass flow gain factor.

However, we were not able to fully explain the mechanism of the influence of the simple modification of the inducer upstream housing on the rotating cavitation. Experiments mainly employing visual observations were newly conducted using the inducer test facility at the Kakuda Research Center of the National Aerospace Laboratory to clarify the mechanism by which the simple modification of the inducer upstream housing suppressed rotating cavitation in the LE-7 LOX main pump.

Apparatus and Procedure

Test Inducer and Housings

The inducer utilized in this experiment had dimensions similar to those of the inducer of the LE-7 LOX main pump. The inducer is shown in Fig. 1. The design characteristics of the test inducer are as follows: inlet flow coefficient, 0.0775; outlet flow coefficient, 0.094; inlet tip diameter, 127.4 mm; inlet hub ratio, 0.3; outlet tip diameter, 127.4 mm; outlet hub ratio, 0.5; inlet tip blade angle, 7.25 deg; outlet tip blade angle, 9.25 deg; tip solidity, 2.0; and leading-edge sweep, swept-back. The inducer has three swept-back helical, cambered blades.

Three types of inducer housings are shown in Fig. 2 and Table 1. The original housing (housing E*) that caused rotating cavitation becomes slightly narrow in diameter at the leading edge of the inducer inlet. On the other hand, housing C*, the modified housing, becomes slightly wider in diameter at the

Presented as Paper 96-2674 at the AIAA/ASME/SAE/ASEE 32nd Joint Propulsion Conference, Lake Buena Vista, FL, July 1–3, 1996; received July 28, 1996; revision received Feb. 10, 1997; accepted for publication Feb. 14, 1997.

*Senior Researcher, Kakuda Research Center.
†Senior Researcher, Kakuda Research Center. Member AIAA.
‡Researcher, Kakuda Research Center.
§Professor, Institute of Fluid Science. Senior Member AIAA.
¶Professor, Engineering Science. Member AIAA.

Table 1 Dimensions of inducer casings

Inducer housing	D_1	D_2	D_t
Modified (C*)	ϕ131	ϕ128.85	ϕ127.4
Original (E*)	ϕ127.6	ϕ128.85	ϕ127.4
Straight (B*)	ϕ129.1	ϕ129.1	ϕ127.4

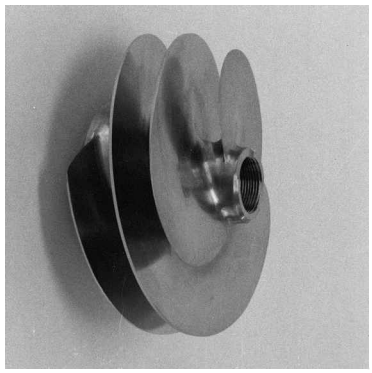

Fig. 1 Inducer tested.

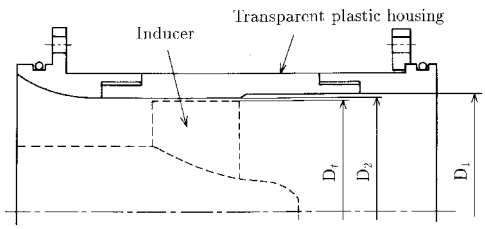

Fig. 2 Configurations of inducer housing.

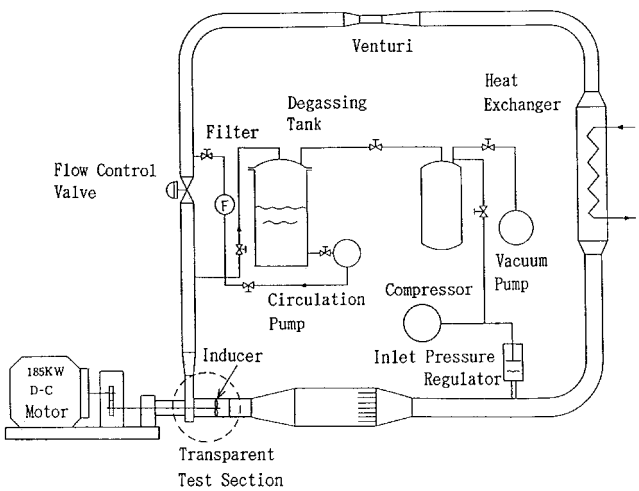

Fig. 3 Cavitation tunnel test facility.

leading edge of the inducer inlet. Housing B*, straight housing, has a constant diameter from upstream to downstream of the inducer. However, the tip clearance in the case of housing B* is a little larger than those in the cases of housing C* and E*. These three types of casings are all manufactured from transparent plastic for visual observations.

Test Facility and Test Section

The present experiment was performed in a closed-loop inducer test facility, a schematic diagram of which is shown in Fig. 3. The inducer is powered by a 185-kW dc motor through a multiplying gear box. The rotational speed of the motor is held constant by an electrical control system. The facility can reduce the gas content of water to approximately 4 ppm in weight, which results in distinct pictures of cavitation in the inducer.

The mean flow rate was measured by means of a venturi meter. Dynamic pressures were measured by pressure transducers utilizing the semiconductor piezo resistance effect. The dynamic pressure transducers were installed in the inducer housing approximately 100 mm upstream and 40 mm downstream of the inducer's leading and trailing edges, respectively. Displacement of the shaft was measured by an eddy-current-type sensor, which was installed behind a ball bearing on the inducer side as shown in Fig. 4. The dynamic pressures and the shaft vibrations were recorded with an FM data recorder, and spectrum analyses were conducted by a fast Fourier transform analyzer.

Procedure

The water was degasified before every test. The water temperature was held constant using a heat exchanger during all operations. Data were taken in groups of constant shaft speeds of 7000 or 10,000 rpm and a constant flow rate for each rotational speed, while the inducer inlet pressure was varied from high to low using the inlet pressure regulator shown in Fig. 3.

A stroboscopic light was triggered by the magnetic pulse pick-up on the shaft so that the motion of the inducers appeared to stop and the same blade could be observed. High-speed filming was done using a continuous light source, at a framing rate of 7000 frames per second. A view of the test section including the high-speed camera and light sources is shown in Fig. 5.

Results and Discussion

Various Modes of Cavitating Flow

Figure 6 presents some regions in which various modes of cavitating flow in an inducer were observed with the original inducer housing (housing E*), which was closely related not only to unsynchronous shaft vibrations, but also to pressure fluctuations, mainly in the inducer inlet. These regions were obtained from data of shaft vibrations, inlet dynamic pressures, and high-speed film.

Mode ② in Fig. 6 is forward-rotating cavitation, which was one of the most troublesome problems in the development of

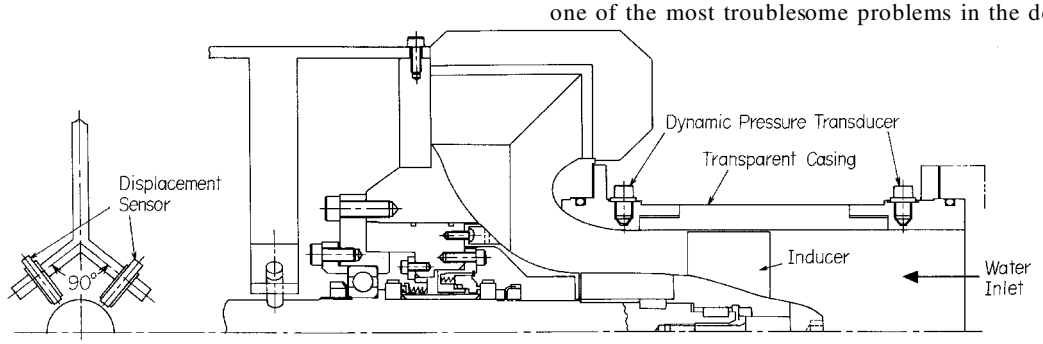

Fig. 4 Positions of dynamic pressure and shaft displacement sensors.

the LE-7 LOX main pump. Figure 7 presents the fluctuation of the tip vortex cavity area of three blades with time in the rotating cavitation with the rotational frequency of 138 Hz. The data were obtained from high-speed film using a photograph analyzer. Although this method probably resulted in some error because of the obscurity of the end of the cavity, it yielded information that was very useful for the following discussion. The larger cavity area clearly moved around the periphery of the inducer inlet with a constant rotating speed that was faster than the inducer rotating speed, just the same as was the case in our previous report.[1,2] This fact shows that an area that causes rotating cavitation moves around the periphery of the inducer inlet with a rotating speed that is faster than the inducer rotating speed, which subjects the inducer to radial forces and results in supersynchronous shaft vibrations.

Figure 8a shows a spectrum analysis of inlet dynamic pressure. The frequency of forward-rotating cavitation ω_{c2} decreased with the decrease of the cavitation number. When the forward-rotating cavitation occurred, some vibrations with a frequency different from ω_{c2} appeared as a result of the mutual interference between ω_{c2} and ω_s. Here, ω_s is the frequency of the shaft rotating speed. In Fig. 8a, $(\omega_{c2} - \omega_s)$ and 3 $(\omega_{c2} - \omega_s)$ were observed. The fact that the frequencies were described by the difference between ω_{c2} and ω_s clearly suggested that the direction of forward-rotating cavitation was just the same as that of inducer-rotating blades.

The frequency of 159 Hz (ω_{c1}) in Fig. 8a was considered to be caused by backward-rotating cavitation based on the following evidence. Backward-rotating cavitation was already predicted by the theoretical analysis.[7] The frequencies of 276 and 827 Hz in Fig. 8b described by $(\omega_{c1} + \omega_s)$ and 3 $(\omega_{c1} + \omega_s)$ were definitely observed. Because the frequencies were described by forms of the sum of ω_{c1} and ω_s, this clearly suggested that the direction of backward-rotating cavitation was opposite that of rotating blades. Furthermore, it was very interesting that the frequency of 297 Hz (the sum of $\omega_{c1} + \omega_{c2}$) appeared when the backward- and forward-rotating cavitation coexisted.

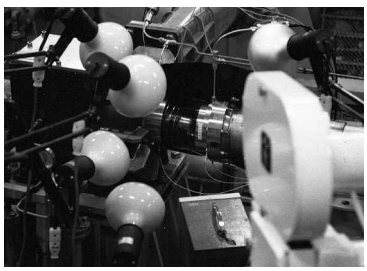

Fig. 5 View of test section including high-speed camera and light sources.

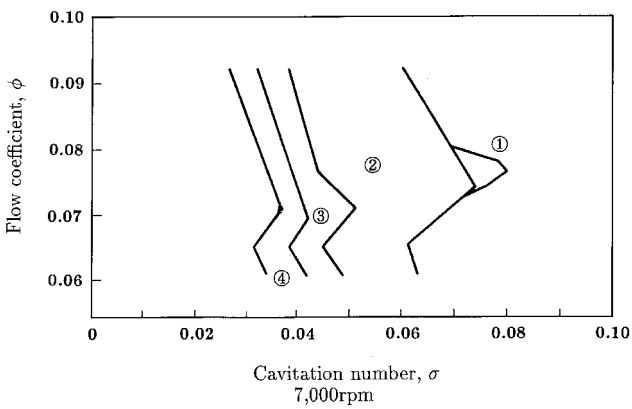

Fig. 6 Various modes of cavitating flow. ①, backward-rotating cavitation; ②, forward-rotating cavitation; ③, attached cavitation; and ④, low cycle oscillations.

Figure 9 shows the relationship between shaft revolution, that is time, and tip vortex cavity length with three blades when the oscillation of 159 Hz was observed in both the inlet dynamic pressure and the shaft displacement. The data were measured from high-speed film for a time interval shorter than those in Fig. 7. The solid, dotted, and chain sinusoidal lines in Figs. 9a and 9b are based on the assumption that the cavity length fluctuations were caused by backward-rotating cavitation and by forward-rotating cavitation, both with a rotational frequency of 159 Hz.

The frequency of the assumed cavity length fluctuation with one blade in Figs. 9a and 9b results in 276 Hz, that is $(\omega_{c1} + \omega_s)$, and 42 Hz, that is $(\omega_{c1} - \omega_s)$, respectively. In Figs. 9a and 9b, the longer cavities with three lines are assumed to propagate in the direction of blade numbers 1, 2, 3 and 1, 3, 2, respectively. From comparison of Fig. 9a to Fig. 9b, it was found that the data measured from the high-speed movie film were in much better agreement with the three assumed lines in Fig. 9a. Therefore, we concluded that the rotating cavitation of 159 Hz was backward-rotating cavitation.

Measurement of the phase difference between two shaft displacement sensors clarified the propagating direction of rotating cavitation. The two sensors measured a shaft vibration with a phase difference of 90 deg because the sensors were installed as shown in Fig. 4. If we assume ideal backward-rotating cav-

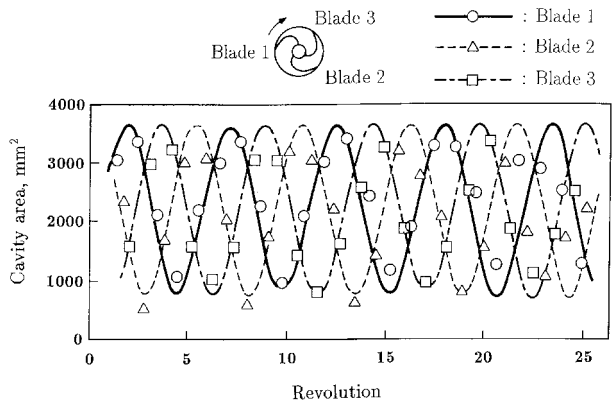

Fig. 7 Cavity area fluctuation during forward-rotating cavitation.

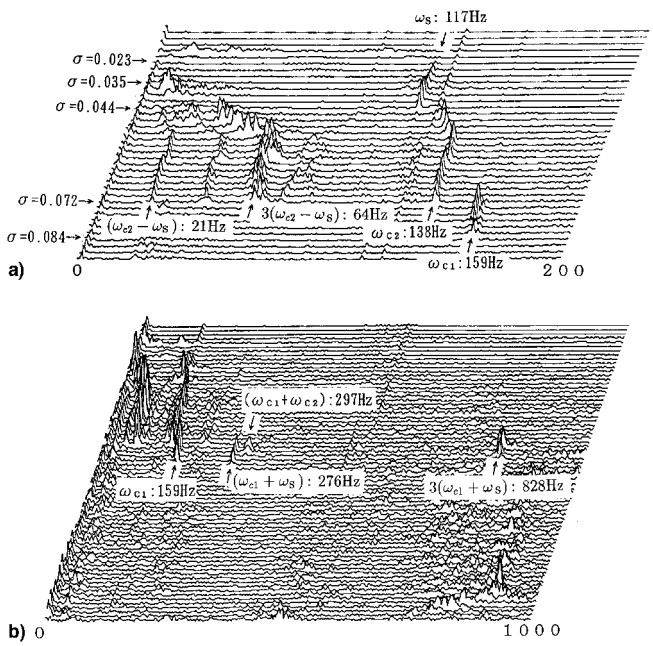

Fig. 8 Spectrum analysis of inlet dynamic pressure: a) 0 ~ 200 and b) 0 ~ 1000 Hz.

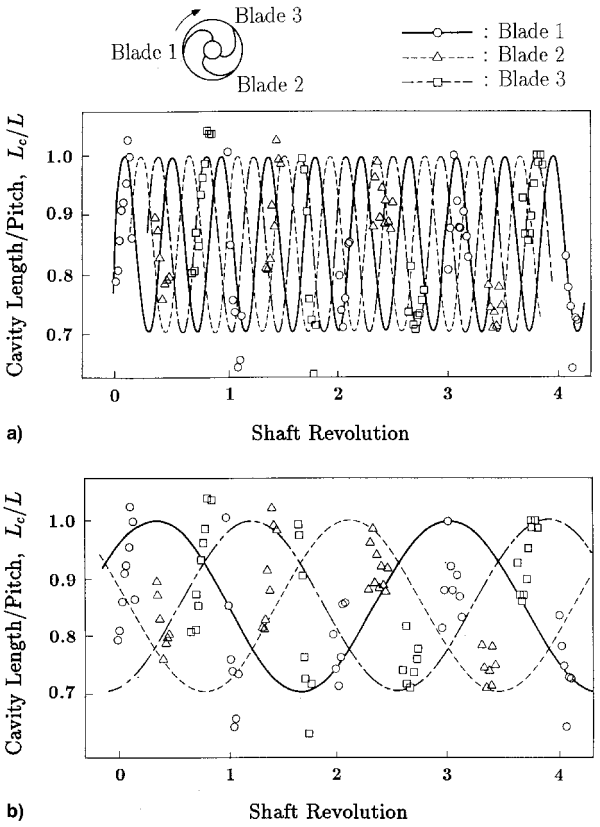

Fig. 9 Oscillation of cavity length; with assumption of a) backward- and b) forward-rotating cavitations.

itation with the frequency of 159 Hz, the signal of the D-2 sensor should be 90 deg after that of the D-1 sensor. The phase delay of the rotating cavitation of 159 Hz was 69.9 deg, which agreed with the ideal phase delay mentioned earlier. Incidentally, with the forward-rotating cavitation of 138 Hz, the signal of the D-2 sensor was 70.3 deg ahead of the D-1 sensor, which also agreed well with the expected phase difference of 90 deg. Furthermore, spectrum analyses of the dynamic pressures gave almost the same results as those of the shaft vibration mentioned earlier.

Mode ③ in Fig. 6 presents attached cavitation or steady asymmetric cavitation.[1,2] This mode can be considered to be a kind of rotating cavitation, the rotating speed of which is just the same as inducer rotating speed. This mode also occurred in the LE-7 LOX main pump inducer, which brought about large synchronous shaft vibration.

Mode ④ in Fig. 6 is a low-cycle oscillation that is surge caused by cavitation (cavitation surge). In this cavitation surge, severe pressure oscillations occurred both upstream and downstream of the inducer. All of the cavities on three blades did not oscillate in unison, but steady asymmetric cavitation (mode ③ in Fig. 6) had a strong influence on this cavitation surge. This characteristic was very different from the previous experimental results[1,2] in which all cavities on three blades oscillated almost in unison.

Influence of Inducer Housing Geometries

Figure 10 presents the regions in which some modes of cavitating flows occurred with the modified inducer housing (housing C*) and straight inducer housing (housing B*). Comparison of this figure with Fig. 6 of the original inducer housing clarified the difference of influence of these three inducer housing geometries on cavitating flows, in particular tip vortex cavitating flows. Figure 10 clearly shows that both the modified and straight inducer housings shifted the regions of the unsteady cavitating flows, such as rotating cavitation and attached cavitation, to higher flow rates. It can be considered that the same shifting suppressed rotating cavitation in the LE-7 LOX main pump inducer (the design flow coefficient was 0.078 for both the inducers of the present test and the LE-7 LOX main pump).

Figure 11 shows photographs of tip vortex cavitating flows with the three inducer housings. Since these photographs were taken using stroboscopic light, they show the time-averaged cavitating flows. In the cases of the modified and the straight inducer housings, the tip vortex cavitation stretched much more upstream than in the case of the original inducer housing. That is, the backflow from the tip clearance was more pronounced in the case of the modified and straight inducer housing than in the case of the original inducer housing. This increase of backflow cavitation is considered to be closely related to the suppression of rotating cavitation. Control of backflow at the inducer inlet at low flow rate was reported by Sloteman et al.[8] and Jakobsen.[9] In the present paper, however, we cannot clarify the relationship between the control of backflow at the low flow rate and the growth of backflow cavitation in Fig. 11.

Based on his experimental results, Shimura[10] reported that the suppression of rotating cavitation of the LE-7 main pump inducer was caused by changes in the cavitation compliance and mass flow gain factor. The increase of tip vortex cavitation with backflow in the present experiment seems to be related to Shimura's suggestion.[10]

Figure 12 presents the shaft vibrations measured by the displacement sensors, the amplitudes of which were increased by rotating cavitation. The flow coefficients for the three cases were the same, $\phi = 0.0885$. The straight and original inducer housings showed almost the same large magnitude of vibration amplitude, while the modified inducer housing showed quite a small amplitude. In addition to its other positive qualities, men-

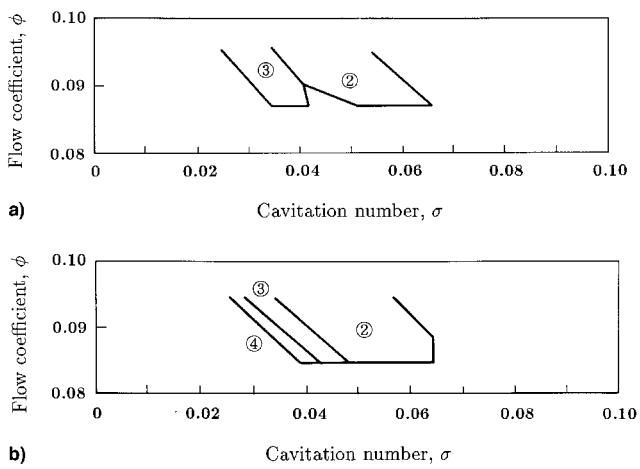

Fig. 10 Modes of cavitating flow: a) modified and b) straight casings. ①, backward-rotating cavitation; ②, forward-rotating cavitation; ③, attached cavitation; and ④, low-cycle oscillations.

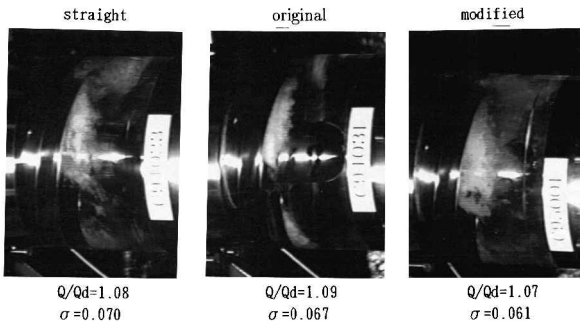

Fig. 11 Photographs of tip vortex cavitating flows.

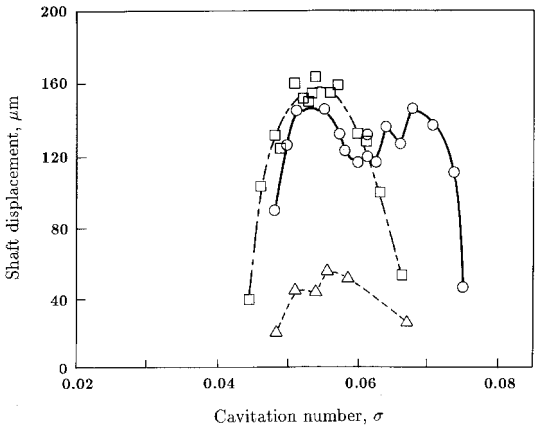

Fig. 12 Comparison of magnitude of shaft displacements with different casing by rotating cavitation at f = 0.0885. ——○—— original, - - - -△- - - - modified, and —·—□—·— straight.

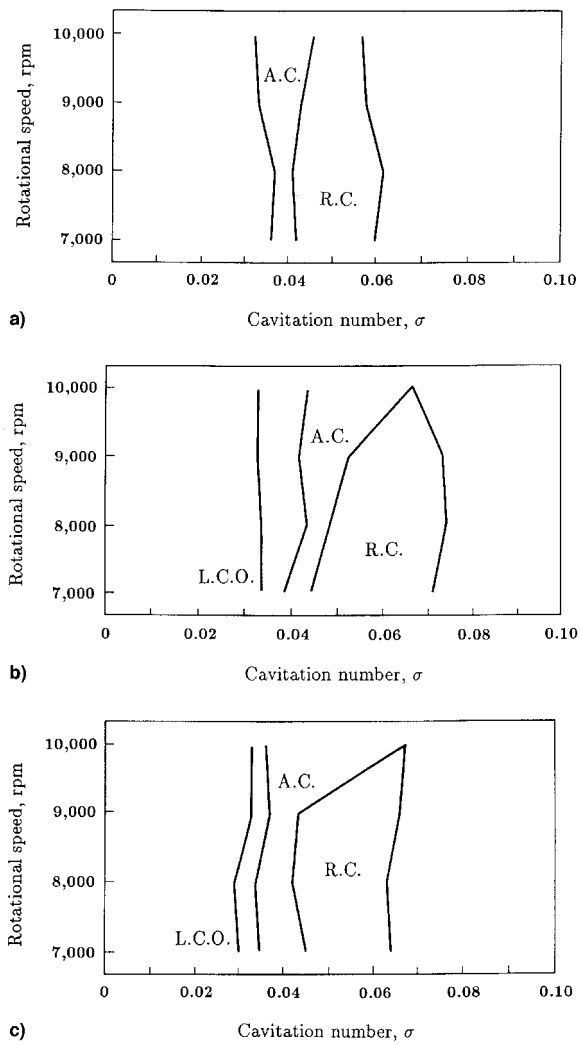

Fig. 13 Influence of rotational speeds on modes of cavitating flows: a) modified casing at f = 0.089, b) original casing at f = 0.078, and c) straight casing at f = 0.090.

tioned earlier, the modified inducer housing is also considered to weaken the phenomenon of rotating cavitation.

Influence of Rotational Speeds

Figure 13 presents the influence of rotational speed on the modes of cavitating flows. It was very small with the modified inducer housing. With the original and straight inducer housings, rotating cavitation changed to attached cavitation even at the same cavitation number with the increase of rotational speed. This noticeable difference is considered to be a result of the difference in the magnitude of shaft vibration already shown in Fig. 12. The nonuniform distribution of tip vortex cavitation around the periphery of the inducer inlet seemed to increase with the increase of shaft vibration amplitude. This tendency was more pronounced with the straight and original inducer housings. The nonuniform distribution of tip vortex cavitation is considered to be closely related to the change from rotating cavitation to attached cavitation, but we cannot fully explain the mechanism.

However, it can be concluded that the modified inducer housing was highly effective in preventing rotating cavitation from changing to attached cavitation that would have resulted in greatly increased synchronous shaft vibration.

Concluding Remarks

Although suppression of rotating cavitation was achieved by a simple modification of the inducer upstream housing in the development of the LE-7 LOX main pump, we were not, however, able to fully explain the mechanism of the suppression.

New experiments were conducted using an inducer similar to that of the LE-7 LOX main pump and a water tunnel to clarify the relationship between the occurrence of various modes of cavitating flow, including rotating cavitation, and the geometries of the inducer upstream housing. Major results of this work are as follows.

Maps of modes of unsteady cavitating flow were obtained. From these maps it was clarified that the modified inducer housing shifted the region in which the unsteady cavitating flows (such as rotating cavitation and attached cavitation) occurred, to higher flow rates above the design flow rate. This result explained the suppression of rotating and attached cavitation by the modified inducer housing of the LE-7 LOX main pump.

Visual observations showed that backflow cavitation at the tip in the case of the modified and straight inducer housings was more pronounced than with the original inducer housing. This increase of backflow cavitation is considered to be closely related to the suppression of rotating cavitation.

The modes of cavitating flow with the straight and original inducer housings were affected by rotational speed. This is because of the increase of the nonuniform distribution of the tip vortex cavitation around the periphery of the inducer inlet caused by the increase in the amplitude of the shaft vibrations resulting from severe rotating cavitation.

Appendix: Suppression of Rotating Cavitation with the LE-7 LOX Main Pump Inducer

Figure A1 presents the mechanical configuration of the LE-7 LOX turbopump. It consists of a main pump and a preburner pump that are driven by a single-stage gas turbine. Design parameters of the LE-7 main pump that has a single-stage impeller with a three-bladed, cambered inducer are rotational speed, 20,000 rpm; main pump = required NPSH, 30 m; mass flow, 229.1 kg/s; pressure rise, 20.9 MPa; and efficiency, 75%. The major design parameters of the inducer are presented as follows: rotational speed N, 20,000 rpm; required NPSH, 30.0 m; suction specific speed S, 2.10 m, m^3/s, s^{-1}; cavitation number σ, 0.017; number of blades, 3; inlet flow coefficient ϕ_1 (values for 1.07 times the quantity of nominal flow), 0.083; outlet flow coefficient ϕ_2 (values for 1.07 times the quantity of nominal flow), 0.104; inducer head coefficient Ψ (values for 1.07 times the quantity of nominal flow), 0.097; tip diameter D_t, 149.8 mm; inlet tip blade angle β_{t1}, 7.50 deg; and outlet tip blade angle β_{t2}, 9.50 deg. A comparatively large sweep-back was necessary to decrease high stresses at the hub near the leading edge.

In the tests of not only the LE-7 LOX turbopump alone, but also of the LE-7 engine system, the original inducer housing

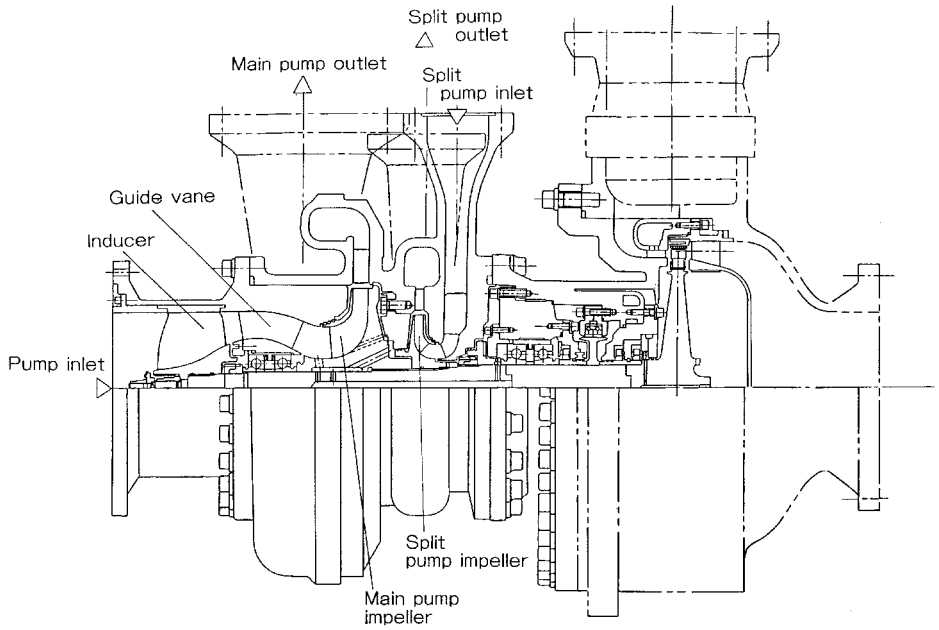

Fig. A1 LE-7 LOX turbopump.

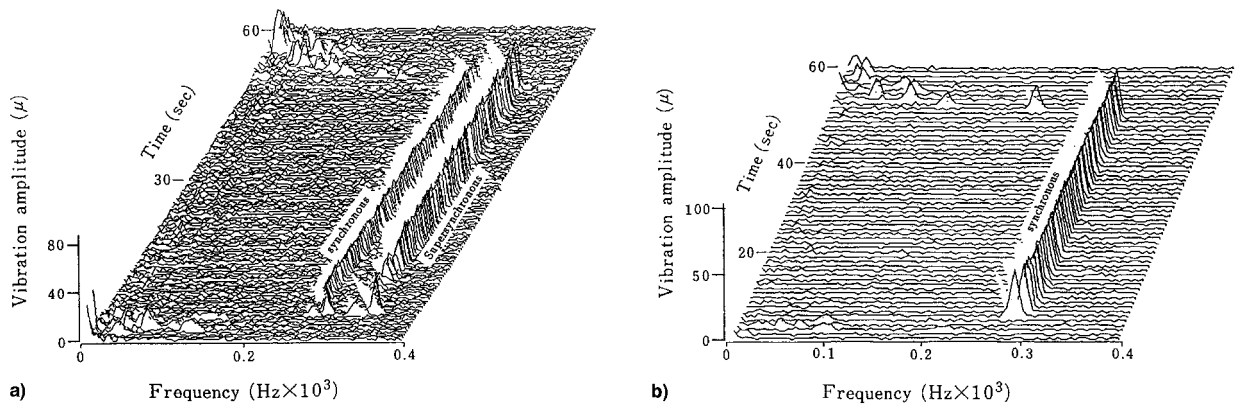

Fig. A2 Spectrum analysis of the displacement of LE-7 main pump impeller. a) original and b) modified inducer housings.

Table A1 Dimensions of inducer housings

Housing	Inside diameter of upstream housing D_1, mm	Inside diameter of first half of liner D_2, mm	Inside diameter of latter half of liner D_3, mm
A	150.8	150.8	151.4
B	151.3	151.3	151.3
C	153.0	151.3	151.3
D	149.8	150.8	150.8
E	149.8	151.8	151.8

(housing E) resulted in supersynchronous shaft vibrations caused by rotating cavitation in the inducer.

Figure A2a presents a spectrum analysis of the displacement of the main pump impeller in the LE-7 engine test using inducer housing A. From comparison with the previous reports we concluded that this supersynchronous vibration was caused by rotating cavitation in the inducer. It was also conjectured that rotating cavitation might be closely related to the tip vortex cavitation of the inducer. Some efforts were made to influence the tip vortex cavitation. We were able to find an inducer housing (housing C) that becomes slightly wider in diameter at the leading edge of the inducer inlet upstream, which almost completely suppressed the rotation cavitation as shown in Fig. A2b. The dimensions and geometries of the original and modified inducer housings are shown in Table A1 and Fig. A3, respectively.

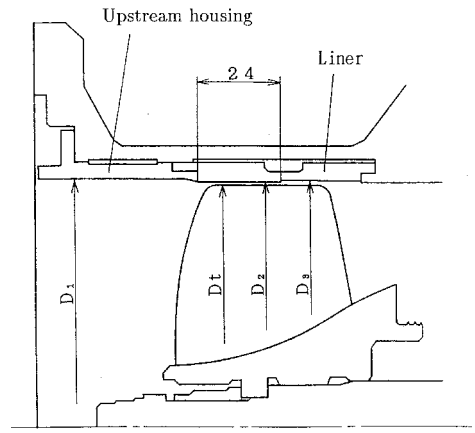

Fig. A3 Geometries of inducer housings.

Though we could fortunately solve the problem of supersynchronous shaft vibrations, we were not fully able to explain the mechanism of the influence of the simple modification of the inducer upstream housing on suppression of rotating cavitation.

References

[1]Kamijo, K., Shimura, T., and Watanabe, M., "An Experimental Investigation of Cavitating Inducer Instability," 77-WA/FE-14, American Society of Mechanical Engineers Winter Annual Meeting, Atlanta, GA, Nov. 1977.

[2]Kamijo, K., Shimura, T., and Watanabe, M., "A Visual Observation of Cavitating Inducer Instability," National Aerospace Lab. (Japan), Rept. TR-598T, May 1980.

[3]Acosta, A. J., "An Experimental Study of Cavitating Inducer," *Proceedings of the 2nd O.N.R. Symposium on Naval Hydrodynamic*, ACR-38, Washington, DC, Aug. 1958, pp. 537–557.

[4]Rosenman, W., "Experimental Investigations of Hydrodynamically Induced Shaft Forces with a Three Bladed Inducer," *Proceedings of the Symposium on Cavitation in Fluid Machinery, American Society of Mechanical Engineers, Winter Annual Meeting*, American Society of Mechanical Engineers, New York, 1965, pp. 172–195.

[5]Soltis, R. F., "Some Visual Observations of Cavitation in Rotating Machinery," NASA TND-2681, July 1965.

[6]Kamijo, K., Yoshida, M., and Watanabe, M., "Hydraulic and Mechanical Performance of the LE-7 LOX Pump Inducer," *Journal of Propulsion and Power*, Vol. 9, No. 6, 1993, pp. 819–826.

[7]Tsujimoto, Y., Kamijo, K., and Yoshida, Y., "A Theoretical Analysis of Rotating Cavitation in Inducers," *Journal of Fluids Engineering*, Vol. 115, No. 1, 1993, pp. 135–141.

[8]Sloteman, D. P., Cooper, P., and Dussord, J. L., "Control of Backflow at the Inlets of Centrifugal Pumps and Inducers," *Proceedings of the 1st International Pump Symposium*, Texas A&M Univ., College Station, TX, 1984, pp. 9–22.

[9]Jakobsen, J. K., "Liquid Rocket Engine Turbopump Inducers," NASA SP-8052, May 1971.

[10]Shimura, T., "The Effects of Geometry in the Dynamic Response of the Cavitating LE-7 LOX Pump," *Journal of Propulsion and Power*, Vol. 11, No. 2, 1995, pp. 330–336.